Processing and Characterization of Ultrathin Carbon Coatings on Glass

Hoikwan Lee, Ramakrishnan Rajagopalan, Joshua Robinson, and Carlo G. Pantano*

Materials Research Institute, The Pennsylvania State University, University Park, Pennsylvania 16802

ABSTRACT Ultrathin carbon layers, on the order of 3−6 nm in thickness, were formed on glass substrates by spin coating and pyrolysis of polymer precursors. The organic precursors used were poly(furfuryl alcohol), coal tar pitch, and a photoresist. The carbon coatings were characterized by ellipsometry, optical profilometry, water contact angle, confocal Raman spectroscopy, UV−vis spectroscopy, and atomic force microscopy. We also report the transparency, hydrophobicity, friction, weathering resistance, and electrical conductivity of the carbon-coated glass. The results reveal that up to 97% transparent, ultrathin carbon films could be formed on glass substrates with a root-mean-square roughness of less than ∼0.3 nm. This carbon layer modified the otherwise hydrophilic surface of the glass to yield a water contact angle of 85°. The coatings were also found to provide a water barrier against weathering under hot and humid conditions. A 4.5-nm-thick carbon film on glass had a sheet resistance of 55.6 kΩ m and a conductivity of 40 S/cm.

KEYWORDS: pyrolysis • carbonization • ultrathin carbon layer • graphite structure • carbon coating

1. INTRODUCTION

Carbon has several different allotropic forms such as graphite (1, 2), nanotubes (3, 4), fullerenes (5), diamond (6, 7), nanoporous carbon (8, 9), amorphous carbon (10, 11), etc., that exhibit a broad range of properties including electrical conductivity, thermal conductivity, porosity, and surface area. In recent times, the two-dimensional (2D) single-layer graphene carbon structure has received considerable interest primarily because of its interesting electrical properties (2, 12−16). This single-layer graphene sheet is also expected to be transparent, hermetic to oxygen and water, and hydrophobic, and so it could be an interesting coating material for glass (17). Presently, the synthesis and deposition of graphene is an active and very challenging area of research, and there is no method yet developed for direct vapor deposition on glass. Alternatively, techniques such as mechanical exfoliation of graphite to create graphene flakes, followed by dispersion and spin-coating of the nanoparticulate graphene flakes or graphene oxide, are being developed for coating glass (18−22).

Carbonization of a graphitizing polymer is another alternative, being explored here, for preparing carbon thin films with a graphitic structure on glass (8, 23−26). Although the formation of a continuous single layer of graphene by this process is somewhat unrealistic at the present time, a nanocomposite thin film of graphene and amorphous carbon would be worthy of evaluation and development. Such a carbon film could be formed on selected glass substrates (even in manufacturing) by coating with a polymer precursor, followed by pyrolysis to yield value-added properties for glass such as hydrophobicity (27, 28), adhesion (27), low friction (29, 30), barrier properties (27), transparency (3, 31), and electrical conductivity (10, 11, 31). The formation of a continuous nanocomposite carbon film on glass could enable a broad range of applications that include easy clean surfaces or transparent electrically conductive coatings.

In this investigation, we explore the use of three different organic precursors to deposit a uniform, nanoscale layer of carbon on glass surfaces. We report the chemical and physical properties of the deposited carbon layer in detail.

2. EXPERIMENTAL PROCEDURE

2.1. Solution Preparation. Furfuryl alcohol resin in the form of Durez resin no. 16470 [poly(furfuryl alcohol), PFA] from Occidental Chemical Corp., coal tar pitch (CTP) purchased from Koppers Inc., and S1805 photoresist (PR) purchased from Shipley were used as the organic precursors. Soluble fractions of CTP were extracted by using tetrahydrofuran (THF) as the solvent. PFA and CTP were diluted using acetone and THF, respectively, to different concentrations (0.5, 1, 5, and 10 wt %). PR was mixed with a p-type thinner (1:10 by weight). The resultant solutions were well mixed in an ultrasonic bath to obtain complete solubility before spin coating. We chose PFA and PR because they are commercially available resins that have the tendency to cross-link at higher temperatures (>250 °C) and thus are good precursors for the synthesis of nongraphitizing disordered carbons. CTP, on the other hand, is a graphitizing precursor that forms an ordered mesophase at temperatures greater than 450 °C.

2.2. Deposition and Pyrolysis of Solution. Prior to deposition, alkali-free glass substrates (AF45 manufactured by Schott Glass) were cut to the desired size (typically 2.5 × 3.5 cm), followed by cleaning with acetone, isopropyl alcohol, and deionized water. The cleaned substrates were dried with N_2 gas and baked at 200 °C for 10 min on hot plate for dehydration. The glass substrates were coated with the diluted organic precursors using a spin coater operated at a rotational speed of 10K rpm for 45 s under a static dispenser program. The samples were then baked at 115 °C for 3 min using a hot plate. The coated glasses were heat-treated to pyrolyze the organic coatings at 10^{-6}−10^{-7} Torr vacuum in a quartz tube furnace; it was ramped at 2 °C/min to 350 °C and allowed to soak for 4 h, followed by a slow ramp at 1 °C/min to 500 °C and another soak for 4 h to provide enough time for pyrolysis and homo-

* Phone: (1)814-863-2071. Fax: (1) 814-863-8561. E-mail: cgp1@psu.edu.
Received for review January 14, 2009 and accepted March 10, 2009

DOI: 10.1021/am900032p

Table 1. Thickness (nm) of Spin-Coated PFA, CTP, and Photoresist before and after Pyrolysis

organic precursors		ellipsometry: before pyrolysis	ellipsometry: after pyrolysis at 800 °C	optical profilometry after pyrolysis at 800 °C	AFM after pyrolysis at 800 °C
PFA	0.5 wt %	9.60 ± 0.15	3.28 ± 0.04	5.7	4.5
	1 wt %	12.88 ± 0.08	3.38 ± 0.06		
	5 wt %	53.31 ± 0.17	10.04 ± 0.05		
CTP	0.5 wt %	16.68 ± 0.15	3.27 ± 0.13	3.6	3.2
	1 wt %	20.94 ± 0.81	4.60 ± 0.18		
	5 wt %	81.66 ± 1.69	5.77 ± 0.15		
PR	10:1	13.39 ± 0.18	2.68 ± 0.05	4.6	5.1

geneous aromatic carbon formation. The samples were then finally heated at 700−800 °C at 5 °C/min and allowed to soak for 2 h before cooling down at 2 °C/min to room temperature. The final pyrolysis temperature for AF45 glass and silicon wafer substrates was 800 °C, while the carbon films made on float glass were limited to 700 °C in order to prevent thermal deformation of glass.

2.3. Characterization of Carbon-Coated Glass. 2.3.1. ***Thickness Measurement.*** In order to measure the thicknesses of the deposited carbon coatings, we prepared carbon-coated samples using similar process parameters such as the concentration of the precursor and the pyrolysis temperature on both silicon and glass substrates. Ellipsometry (Gaertner L115 ellipsometer; Scientific Co.) was used to measure the thickness of the coated silicon wafers both before and after pyrolysis. In order to measure the thickness of carbon-coated glass, the carbon films were selectively etched using oxygen to create a patterned surface. Three-dimensional (3D) images of the patterned surfaces were taken using both optical profilometry (Wyko NT 1100 profilometer; Veeco Instruments, Inc.) and atomic force microscopy (AFM), and the thickness and uniformity of the coatings on glass were examined.

2.3.2. ***Physical Property Measurements.*** **2.3.2.1.** ***AFM (Morphology and Friction).*** Topography and friction of the carbon coatings were analyzed by AFM (Digital Instruments Dimension 2000 atomic force microscope; Veeco instruments, Inc.). The 2D and 3D morphology as well as roughness of the carbon layer were obtained in tapping mode. To measure the frictional behavior, the contact mode of AFM was used and the frictional properties of the carbon coatings were measured using 3D images of height and friction modes at the boundary between the carbon coating and the pristine glass surface. Furthermore, the quantitative changes in frictional resistance were calculated by using the procedure adopted by Koszewski et al. (32).

2.3.2.2. ***Raman Spectroscopy (Structural Characterization).*** Measurements of Raman spectra were carried out using a confocal Raman (WITec CRM200 spectrometer; WITec Instruments Corp.) with 488-nm wavelength of the excitation laser and a 100× (NA = 0.9) objective scanned in the range of 1100−1850 cm^{-1}. The spectra were curve fitted using a Gaussian function to determine the individual contributions of the D and G peaks of the carbon layer.

2.3.2.3. ***UV−Vis Spectroscopy (Transparency).*** UV−vis spectra of carbon-coated glass were recorded using a Cary 100 UV−vis spectrophotometer (Varian, Inc.). The transmission was measured from 200 to 800 nm for the samples, before and after pyrolysis. As a reference, bare glass and blank measurements in air were used to calibrate the background spectrum.

2.3.2.4. ***Contact Angle (Hydrophobicity).*** To characterize the carbon layer, the contact angle of water on the coated glass surface was measured at ambient temperature using the sessile drop technique. The contact-angle measurement was made at five different locations on the coated sample, and the average value was taken.

2.3.2.5. ***Weathering Resistance.*** In order to do the weathering test, an ultrathin carbon film was formed on float glass, which is susceptible to leaching. Carbon coatings were made using the three precursors by pyrolysis at 700 °C. The effect of the carbon coating on the chemical durability of the glass surface was evaluated at a constant 85% relative humidity and a temperature of 85 °C for several days. The samples prepared using each precursor were removed from the chamber at time intervals of 1, 2, 3, 5, 7, and 10 days, and the surfaces were observed with an optical microscope.

2.3.2.6. ***Electrical Conductivity.*** Characterization of the electrical properties of the thin carbon films was carried out using a two-point probe $I-V$ station designed and fabricated for measuring the electrical resistance as a function of the temperature. The 50-nm-thick gold electrodes, 2 mm × 5 mm, were sputtered on top of the carbon film pyrolyzed on a glass substrate. The resistance and conductivity was calculated from current−voltage curves.

3. RESULTS AND DISCUSSION

The thicknesses of the spin-coated carbon precursor films, before and after pyrolysis, were measured by ellipsometry, optical profilometry, and AFM and are summarized in Table 1. The thicknesses of the coatings after spin coating increase with the concentration of the organic precursors and are in the range of 10−80 nm. During pyrolysis, the polymer decomposes to leave behind a thin carbon layer on the glass surface. The thickness of the pyrolyzed film was in the range of 20−25% of the original thickness for the three precursors. To further confirm the thickness and continuity of the coatings, the carbon-coated surfaces were patterned by using a shadow mask to selectively etch the carbon film with oxygen. Figure 1 shows the 3D representation showing the interface between the coated glass and the etched surface. It can be seen that the ultrathin carbon layer is continuous and has a thickness in the range of 3.6−5.6 nm for all of the pyrolyzed precursors. Likewise, thickness profiles obtained by AFM from these patterned samples confirmed again that these carbon layers are 3−6 nm in thickness.

AFM was also used to study the surface morphology and roughness of the carbon-coated layers. AFM images obtained in tapping mode are displayed in Figure 2a−c. The ultrathin carbon layers are smooth and uniform. The root-mean-square (rms) surface roughnesses of carbon films obtained from PFA and PR were in the range of 0.18−0.22 nm. Comparatively, the CTP-derived carbon coating has a slightly larger surface roughness of ∼0.35 nm.

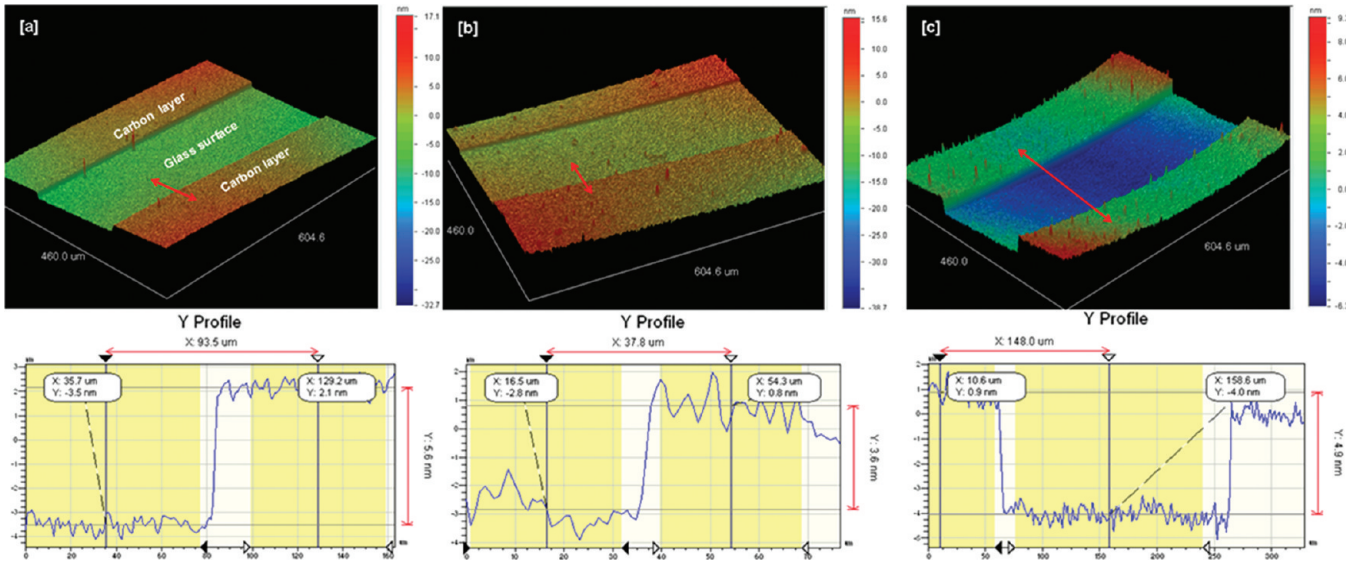

FIGURE 1. 3D image scanned using optical profilometry to measure the thickness of the patterned carbon film deposited on AF45 glass substrate after pyrolysis at 800 °C using spin-coated 0.5 wt % PFA, 0.5 wt % CTP, and PR (10:1) as precursors.

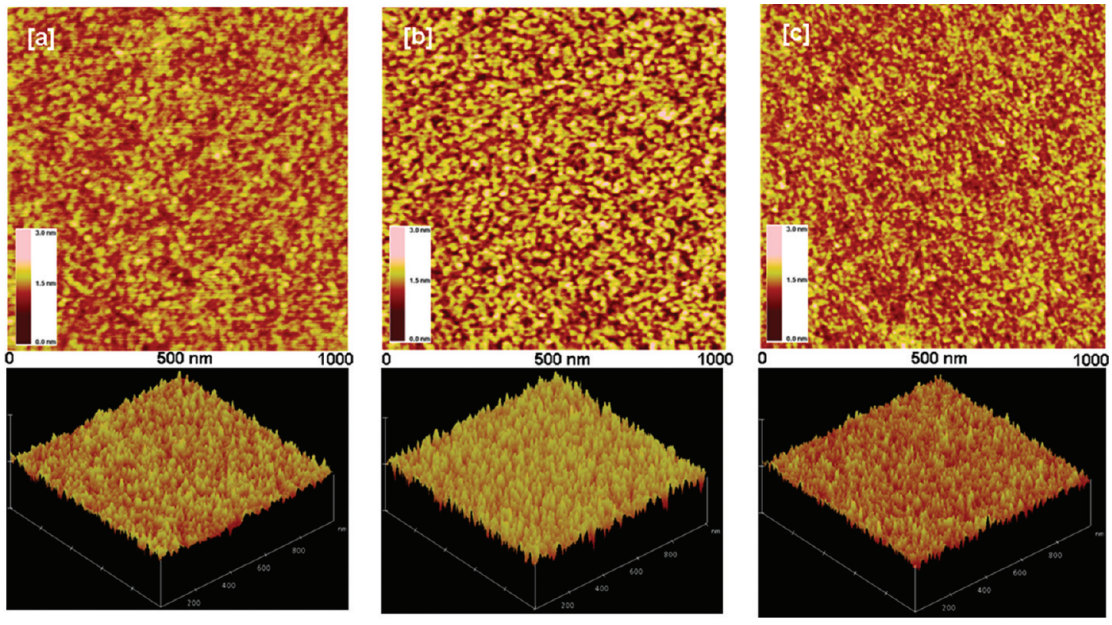

FIGURE 2. AFM topographical images (flattened images and 3D images) (1 μm $\times$ 1 μm) of the deposited carbon layer: (a) 1 wt % PFA, rms roughness = 0.190 $\pm$ 0.027 nm; (b) 5 wt % CTP, rms roughness = 0.293 $\pm$ 0.036 nm; (c) PR (10:1), rms roughness = 0.180 $\pm$ 0.021 nm.

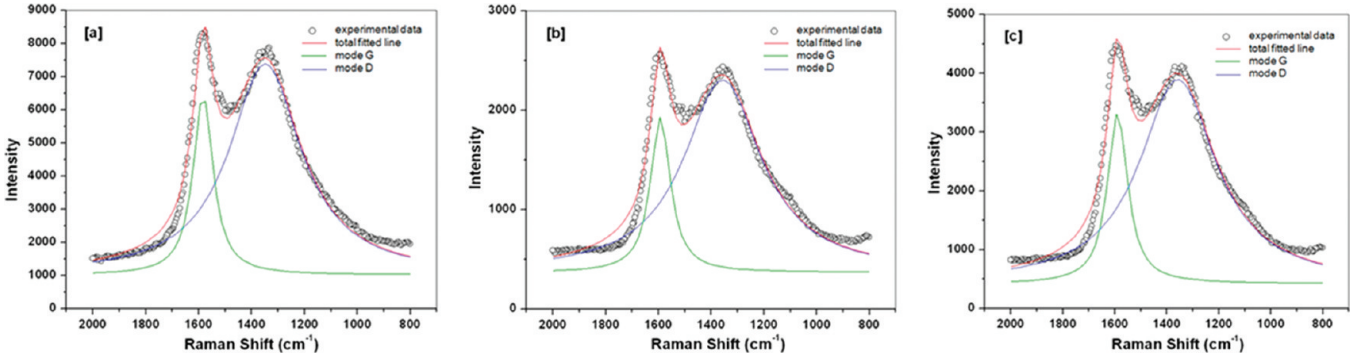

FIGURE 3. Raman spectra of thin carbon layers deposited using (a) 0.5 wt % PFA, (b) 0.5 wt % CTP, and (c) PR (10:1) pyrolyzed at 800 °C.

Figure 3 shows the Raman spectral data experimentally obtained from the carbon-coated glass. The two most intense features are the G peak at 1580 cm^{-1} and the D peak at 1350 cm^{-1}, and these peaks are clearly seen for all of the carbons made using the three organic precursors. The presence of G and D peaks confirms the formation of

Table 2. Raman Intensities of Deconvoluted G and D Peaks for the Carbon-Coated AF45 Glass Pyrolyzed at 800 °C

	intensity			fwhm	
material	I_G	I_D	intensity ratio I_D/I_G	B_G	B_D
0.5 wt % PFA	6280	7738	1.232	89.91	332.29
0.5 wt % CTP	1926	2301	1.195	90.24	359.20
PR (10:1)	3315	3888	1.173	92.80	359.26

polyaromatic carbon on the surface of the glass. The G peak is usually referred to as the Raman-active E_{2g} in-plane vibration mode of polyaromatic domains, while the D peak is assigned to the A_{1g} in-plane breathing mode (33), which is due to the presence of disorder in the structure. The relative peak intensity ratio (I_D/I_G) is correlated to the reciprocal of the crystalline size along the basal plane ($1/L_a$). The relative intensities of the two peaks were measured by deconvoluting the peaks in the Raman spectra. Even though there are differences in the types of precursors, all of the films pyrolyzed at 800 °C show significant amounts of disorder such as edge defects, dangling bonds, etc. In order to understand the structural differences between the three precursors, it is important to anneal the films at much higher temperatures (1000−1500 °C) to induce significant alignment of polyaromatic domains. However, the maximum temperature for these experiments was limited by the softening point of the glass substrate.

Table 2 summarizes the Raman results for the carbons derived from the three precursors. The relative intensities (I_D/I_G) for all three carbons range between 1.173 and 1.232. This corresponds to $L_a \sim 3.6$ nm, which is the case with the most disordered carbons.

The transmittance spectra after pyrolysis are presented in Figure 4. The AF45 glass exhibited a 91% transmittance with respect to air when probed in the visible region of wavelength greater than 400 nm. The transmittance of AF45 glass dramatically decreases below 400 nm because of the UV cutoff at ~300 nm. Among the carbon-coated glasses, CTP-derived carbon-coated glass showed the highest transmittance. This is in good agreement with the thickness measurements, which showed that the CTP-coated glass was the thinnest. In order to better characterize the effects of the carbon film, an AF45 glass substrate was heat-treated at 800 °C to provide reference spectra, as shown in Figure 4b. This makes it possible to identify the absorbance at 250 nm, which is characteristic of these, and most, carbonaceous materials (31, 34). All of the carbon-coated glasses derived from different organic precursors showed absorption in the range of 250−300 nm after pyrolysis. Figure 4c shows the transmittance at 650 nm as a function of the thicknesses of the deposited carbon layers. Both CTP- and PFA-derived carbon layers showed a decrease in the transmittance with increased thicknesses. Depending upon the concentration of PFA or CTP, it was possible to make very thin transparent carbon films from both precursors. However, the PFA-derived carbon films became considerably thicker with an increase in the concentration of the precursor, while CTP showed a gradual increase in the thickness with increased concentration. The transmittance was almost 97% in the visible region for the carbon-coated glasses with thicknesses on the order of 3−4 nm synthesized using both PFA and CTP. As the thickness increased beyond 5 nm, the transmittance dramatically dropped for PFA-derived carbon films (65% at 10 nm).

FIGURE 5. Water contact-angle measurements done on (a) pristine AF45 glass and (b) carbon-coated AF45 glass made using PR (10:1) as the precursor (~5 nm thick).

Table 3. Water Contact Angle on an Organic-Precursor-Coated Glass Surface after Pyrolysis at 800 °C

organic precursors		contact angle of water (deg)	contact angle of the glass surface
PFA	0.5 wt %	80.78 ± 2.55	47.57 ± 2.46
	1 wt %	80.55 ± 3.92	
	5 wt %	79.96 ± 2.39	
CTP	0.5 wt %	79.56 ± 4.22	
	1 wt %	77.34 ± 1.75	
	5 wt %	77.61 ± 1.45	
PR	10:1	85.33 ± 2.19	

The contact angle of water on the freshly cleaned glass substrate (Figure 5a) was 47.56°. Carbon-coated glass showed

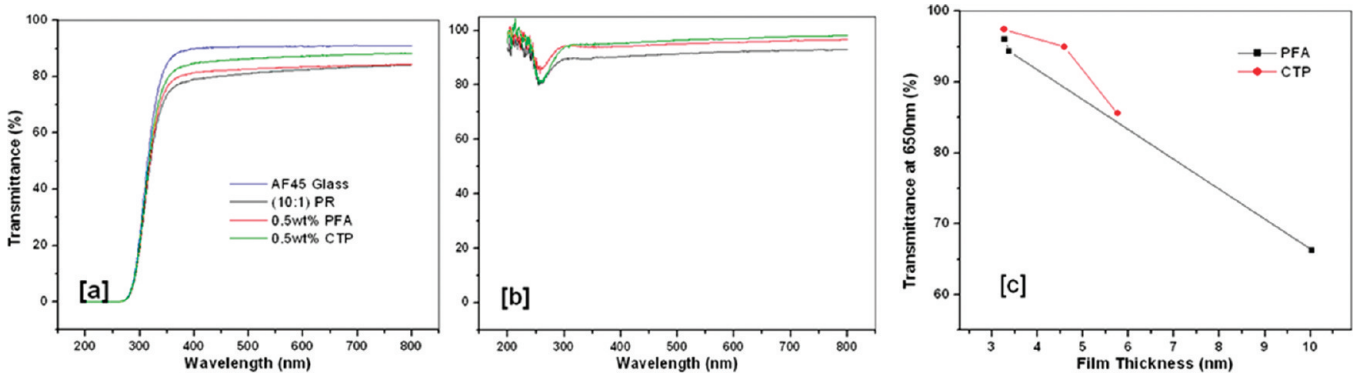

FIGURE 4. Comparison of the transmittance of carbon-coated glasses as measured using UV−vis spectroscopy with respect to (a) air as the reference and (b) the bare glass substrate as the reference. (c) Change in the transmittance as a function of the film thickness of the carbon layer on AF45 glass.

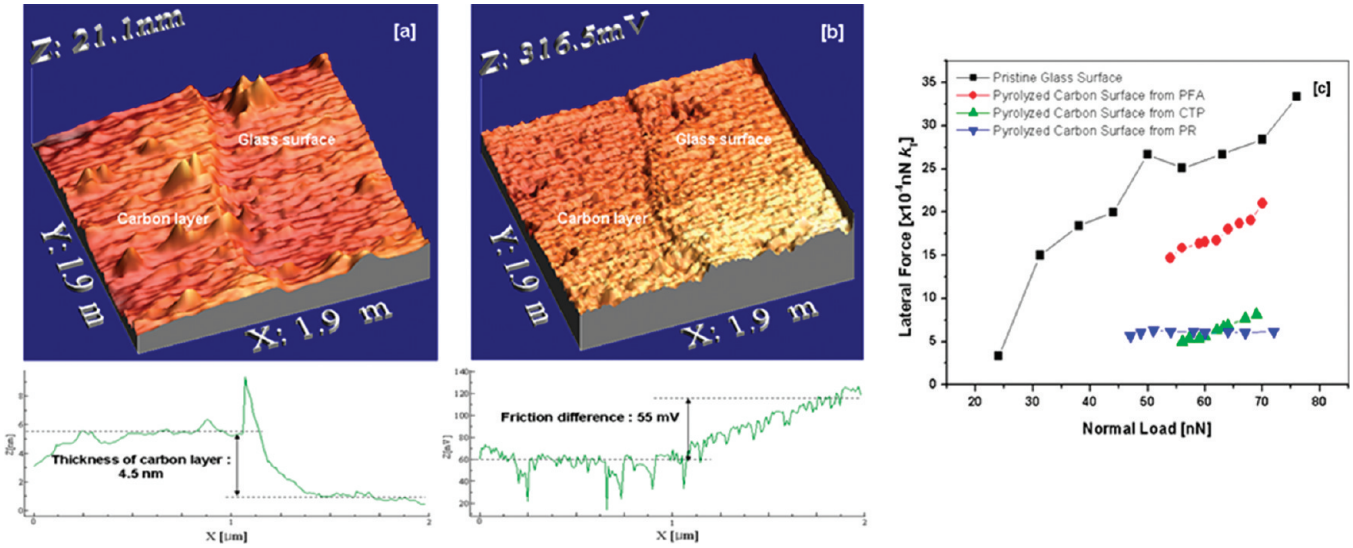

FIGURE 6. (a) Topography, (b) friction profiles, and (c) lateral force vs normal load data measured using AFM FDCs and the torsion loop (K_T: torsion spring constant) on carbon-coated AF45 glass (4.5 nm thick) made using PFA as the precursor.

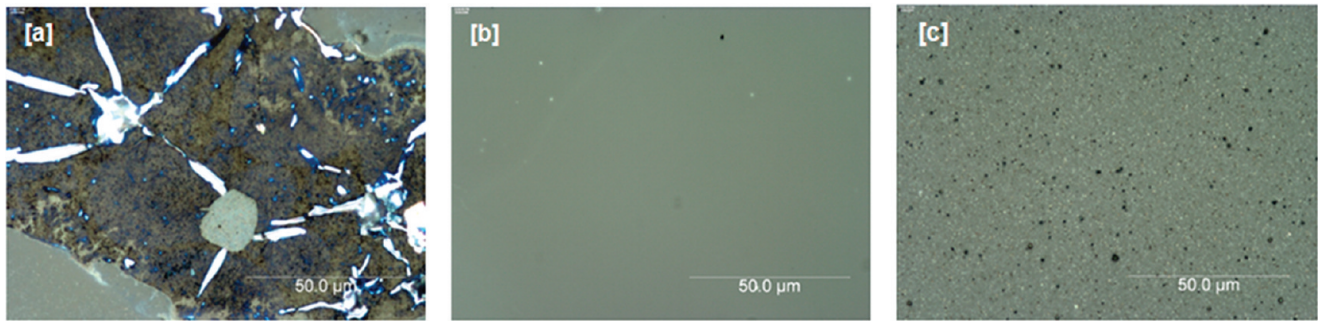

FIGURE 7. Optical micrographs of the glass surfaces exposed to 85 °C and 85% relative humidity for 10 days: (a) pristine float glass; (b) carbon-coated float glass made using PR (10:1) as the precursor; (c) carbon-coated float glass made using a 0.5 wt % CTP solution as the precursor.

a substantial increase in the contact angle. PR-derived carbon (Figure 5b) showed the highest contact angle of 85°, while those of PFA and CTP were 80° and 78°, respectively. Static water contact angles measured on the carbon layers of the PFA, CTP, PR, and pristine glass surface are summarized in Table 3.

Parts a and b of Figure 6 present the topography and friction profiles for the bare and carbon-coated glasses over 1.9 × 1.9 μm^2 scan areas. It is seen that the height image and the frictional force image are complementary to each other. The exposed glass surface has higher frictional resistance compared to the carbon-coated glass surface. In Figure 6c, the lateral force versus normal load for the carbon-coated surface is reported. The normal load and the lateral force have been extracted from the force−distance curve (FDC) and the torsion loop, which is the measured torsion of the cantilever versus relative displacement. As shown in Figure 6, the measured friction value on the carbon-coated surface was 5 times less than that of the bare pristine glass. PR and CTP showed considerably lower frictional resistance (by 2 times) than PFA. Even though Raman studies did not indicate significant structural differences, it is possible that PR and CTP have comparatively more ordered polyaromatic domains than PFA, resulting in increased lubricity. Moreover, PFA-derived carbons are nanoporous in nature, while carbons from CTP are expected to be pore-free (8, 9).

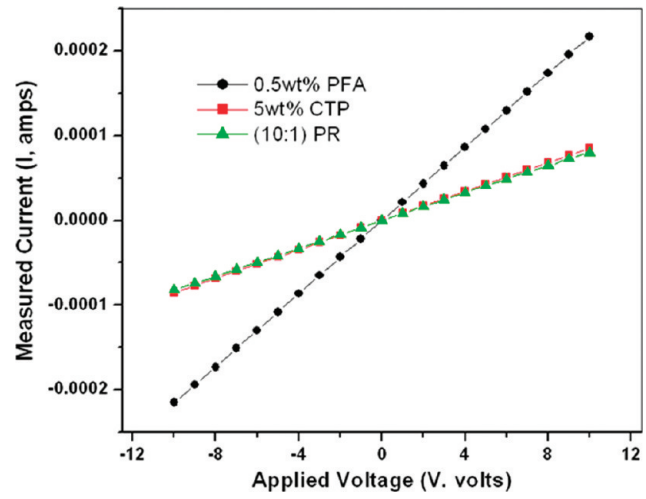

FIGURE 8. Plot of current (I) vs voltage (V) measured using carbon-coated AF45 glass samples derived from 0.5 wt % PFA, 5 wt % CTP, and PR (10:1) as 46, 117, and 123 kΩ, respectively.

The corrosion resistances of the coated glasses were tested under hot and high-humidity conditions. Figure 7

shows the optical micrographs of samples under the influence of this weathering condition for 10 days. The bare surface of this glass was visibly deteriorated, while the carbon-coated glass surfaces (Figure 7b,c) did not appear to exhibit any visible signs of corrosion. This result clearly indicates that the ~5 nm thickness of the carbon layer can provide a water barrier and, thereby, improve significantly the chemical durability of the glass surface.

Figure 8 shows the *I*−*V* characteristics of the pyrolyzed films from the various organic precursors. These carbon films exhibit ohmic behavior (35). The room temperature electrical resistances calculated from the *I*−*V* measurements were 46 kΩ (PFA), 117 kΩ (CTP), and 123 kΩ (PR). The electrical resistance and conductivity were found to vary with the film thickness, and the representative conductivity values measured from these three carbon films were 0.432 × 10^2 S/cm (PFA at 4.5 nm), 0.148 × 10^2 S/cm (CTP at 6 nm), and 0.163 × 10^2 S/cm (PR at 5 nm).

4. SUMMARY

We began this investigation by choosing polymeric precursors such as PFA, PR, and CTP because they can be easily spin-coated on glass substrates. PFA and PR are cross-linking precursors, while CTP is a graphitizing precursor with a significant content of polymer, i.e., hydrocarbons. Upon pyrolysis, all three precursors undergo decomposition, leaving behind a residual carbon film. Because the coatings were formed on glass, we were limited to a pyrolysis temperature of 700−800 °C. Under these conditions, all three precursors yield glassy or disordered carbon. The transformations of the polymer precursors to disordered carbon is described in detail elsewhere (8). During pyrolysis, the precursors undergo transformations to form polyaromatic domains and, in the process, release gases such as water, CO_2, CO, and CH_4. This results in a significant amount of weight loss. Because the polymer precursor film itself was thin, this translates to the formation of ultrathin carbon layers on the order of 3−6 nm in thickness. CTP has the smallest thickness, as confirmed using optical profilometry, UV−vis measurement, and Raman intensity. This is because the percentage yield of carbon from CTP is relatively less than that from PFA or PR. Raman spectroscopy clearly showed evidence for the formation of polyaromatic carbons on the glass surface.

Our goal in this work was to create a very thin uniform layer of carbon on glass that has very high transparency. UV−vis measurements confirmed that the transmittance through the coated glass was almost 97% with respect to pristine glass. We then addressed the question of uniformity of the deposited carbon layer using several approaches. A morphological study using optical profilometry and AFM revealed that the surface roughness was on the order of 0.2−0.35 nm. We further confirmed the uniformity by doing contact-angle measurements at various locations on the glass surface. The contact angle was consistently higher than that of bare glass at all locations, and PR-derived carbon layers showed the highest contact angle of 85°. This value is consistent with the contact-angle measurements reported for bulk carbon substrates. The study of the frictional properties of this layer using AFM showed that the carbon layer is uniform and lower in frictional resistance by almost 5 times as compared to the pristine AF45 glass surface. We also exposed the carbon-coated float glass to severe weathering conditions and found that the ultrathin carbon layer was, in fact, acting as a significant water barrier. The outstanding chemical durability, transparency, and continuity of the thin film make this carbon coating a promising candidate for use as a transparent conductive electrode for selected applications. The sheet resistance and electrical conductivity of the prepared 4.5-nm-thick carbon-coated glass were 55.6 kΩ m and 40 S/cm, respectively.

Acknowledgment. The authors thank the NSF International Materials Institute on New Functionality in Glasses for their support of H.L. as a visiting scholar (Grant DMR-0409588) and the Penn State Site of the NSF NNIN for use of nanofabrication facilities.

REFERENCES AND NOTES

(1) Reich, B. S.; Thomsen, C. *Philos. Trans. R. Soc. London, Ser. A* **2004**, *363*, 2271.
(2) Ferrari, A. C. *Solid State Commun.* **2007**, *143*, 47.
(3) Wu, Z.; Chen, Z.; Du, X.; Logan, J. M.; Sippel, J.; Nikolou, M.; Kamaras, K.; Reynolds, J. R.; Tanner, D. B.; Hebard, A. F.; Rinzler, A. G. *Science* **2004**, *305*, 1273.
(4) Yi, B.; Rajagopalan, R.; Foley, H. C.; Kim, U. J.; Liu, X.; Eklund, P. C. *J. Am. Chem. Soc.* **2006**, *128*, 11307.
(5) Harris, P. J. F. *Philos. Mag.* **2004**, *84*, 3159.
(6) Umeno, M.; Adhikary, S. *Diamond Relat. Mater.* **2005**, *14*, 1973.
(7) Liu, E.; Kwek, H. W. *Thin Solid Films* **2008**, *16*, 5201.
(8) Burket, C. L.; Rajagopalan, R.; Marencic, A. P.; Dronvajjala, K.; Foley, H. C. *Carbon* **2006**, *44*, 2597.
(9) Burket, C. L.; Rajagopalan, R.; Foley, H. C. *Carbon* **2007**, *45*, 2307.
(10) Kumara, L.; Subramanyam, S. V. *Mater. Res. Bull.* **2006**, *41*, 2000.
(11) Wu, Z.; Yang, Y.; Wang, J. *Diamond Relat. Mater.* **2008**, *17*, 118.
(12) Graf, D.; Molitor, F.; Ensslin, K.; Stampfer, C.; Jungen, A.; Hierold, C.; Wirtz, L. *Solid State Commun.* **2007**, *143*, 44.
(13) Ferrari, A. C.; Meyer, J. C.; Scardaci, V.; Casiraghi, C.; Lazzeri, M.; Mauri, F.; Piscanec, S.; Jiang, D.; Novoselov, K. S.; Roth, S.; Geim, A. F. *PRL* **2006**, *97*, 401.
(14) Graf, D.; Molitor, F.; Ensslin, K.; Stampfer, C.; Jungen, A.; Hierold, C.; Wirtz, L. *The European Physical Journal (Special topic)* **2007**, *148*, 171.
(15) Watcharotone, S.; Dikin, D. A.; Stankovich, S.; Piner, R.; Jung, I.; Dommett, G. H. B.; Evmenenko, G.; Wu, S. E.; Chen, S. F.; Liu, C. P.; Nguyen, S. T.; Ruoff, R. S. *Nano Lett.* **2007**, *7*, 1888.
(16) Wang, X.; Zhi, L.; Mullen, K. *Nano Lett.* **2007**, *8*, 323.
(17) Meyer, J. C.; Geim, A. K.; Katsnelson, M. I.; Novoselov, K. S.; Booth, T. J.; Roth, S. *Nature (London)* **2007**, *446*, 60.
(18) Li, D.; Muller, M. B.; Gilje, S.; Kaner, R. B.; Wallace, G. G. *Nat. Nanotechnol.* **2008**, *3*, 101.
(19) McAllister, M. J.; Li, J. L.; Adamson, D. H.; Schniepp, H. C.; Abdala, A. A.; Liu, J.; Margarita, H. A.; Milius, D. L.; Car, R.; Prud'homme, R. K.; Aksay, I. A. *Chem. Mater.* **2007**, *19*, 4396.
(20) Stankovich, S.; Dikin, D. A.; Piner, R. D.; Kohlhaas, K. A.; Kleinhammes, A.; Jia, Y.; Wu, Y.; Nguyen, S. T.; Ruoff, R. S. *Carbon* **2007**, *45*, 1558.
(21) Dikin, D. A.; Stankovich, S.; Zimney, E. J.; Piner, R. D.; Dommett, G. H. B.; Evmenenko, G.; Nguyen, S. T.; Ruoff, R. S. *Nature (London)* **2007**, *448*, 457.
(22) Biswas, S.; Drzal, L. T. *Nano Lett.* **2009**, *9*, 167.
(23) Tanabe, Y.; Yamanaka, J.; Hoshi, K.; Migita, H.; Yasuda, E. *Carbon* **2001**, *39*, 2347.
(24) Wang, Z.; Lu, Z.; Huang, X.; Xue, R.; Chen, L. *Carbon* **1998**, *36*, 51.

(25) Li, G.; Lu, Z.; Huang, B.; Wang, Z.; Huang, H.; Xue, R.; Chen, L. *Solid State Ionics* **1996**, *89*, 327.
(26) Moriyama, R.; Kumagai, H.; Hayashi, J. I.; Yamaguchi, C.; Mondori, J.; Matsui, H.; Chiba, T. *Carbon* **2000**, *38*, 749.
(27) Nimittrakoolchai, O. U.; Supothina, S. *J. Eur. Ceram. Soc.* **2008**, *28*, 947.
(28) Smay, G. L. *J. Am. Ceram. Soc.* **1988**, *71*, C-217.
(29) Ruan, J. A.; Bhushan, B. *J. Appl. Phys.* **1994**, *76*, 8117.
(30) Mathewmate, C.; McClelland, G. M.; Erlandsson, R.; Chiang, S. *Phys. Rev. Lett.* **1987**, *59*, 1942.
(31) Wang, X.; Zhi, L.; Tsao, N.; Tomovic, Z.; Li, J.; Mullen, K. *Angew. Chem., Int. Ed.* **2008**, *47*, 2990.
(32) Koszewski, A.; Rymuza, Z.; Reutheer, F. *Microelectron. Eng.* **2008**, *85*, 1189.
(33) Tuinistra, F.; Koening, J. L. *J. Chem. Phys.* **1970**, *53*, 1126.
(34) Chhowalla, M.; Wang, H.; Sano, N.; Teo, K. B. K.; Lee, S. B.; Amaratunga, G. A. J. *Phys. Rev. Lett.* **2003**, *90*, 155504.
(35) Kumari, L.; Prasad, V.; Subramanyam, S. V. *Carbon* **2003**, *41*, 1841.

AM900032P